J Mol Model (2013) 19:4147–4153
DOI 10.1007/s00894-012-1749-9

ORIGINAL PAPER

Computational investigation of carbon dioxide absorption in alkanolamine solutions

Hidetaka Yamada · Yoichi Matsuzaki · Firoz Chowdhury · Takayuki Higashii

Received: 14 October 2012 / Accepted: 21 December 2012 / Published online: 11 January 2013

Abstract We investigated CO_2 absorption in aqueous alkanolamine solutions using density functional theory with dielectric continuum solvation models (SMD/IEF-PCM and COSMO-RS). We varied the alkyl chain length (m=2, 3, 4) and the alcohol chain length (n=2, 3, 4) in the alkanolamine structures, $H(CH_2)_mNH(CH_2)_nOH$. Using the SMD/IEF-PCM/B3LYP/6-311++G(d,p) and COSMO-RS/BP/TZVP levels of theory, our calculations predict that the product of CO_2 absorption (carbamate or bicarbonate) is strongly affected by the alcohol length but does not differ significantly by varying the alkyl chain length. This prediction was confirmed experimentally by ^{13}C-NMR. The observed sensitivity to the alcohol chain length can be attributed to hydrogen bonding effects. The intramolecular hydrogen bonds of HN · · · HO, NH_2^+ · · · OH, and $NCOO^-$ · · · HO induce ring structure formation in neutral alkanolamines, protonated alkanolamines, and carbamate anions, respectively. The results from our studies demonstrate that intramolecular hydrogen bonds play a key role in CO_2 absorption reactions in aqueous alkanolamine solutions.

Keywords CO_2 absorbent · Density functional theory · Intramolecular hydrogen bond · Nuclear magnetic resonance · Reaction free energy · Solvation model

H. Yamada (✉) · F. Chowdhury · T. Higashii
Research Institute of Innovative Technology for the Earth,
9-2 Kizugawadai,
Kizugawa, Kyoto 619-0292, Japan
e-mail: hyamada@rite.or.jp

Y. Matsuzaki
Advanced Technology Research Laboratories,
Nippon Steel & Sumitomo Metal Corporation, 20-1 Shintomi,
Futtsu, Chiba 293-8511, Japan

Introduction

Aqueous alkanolamine solutions have been widely used in the removal of acid gases from gas streams. For CO_2 capture on the industrial scale, amine scrubbing is the most promising and currently applicable technology [1]. In this context the CO_2 absorption properties of the alkanolamine solutions have been extensively studied to maximize its capture efficiency and to reduce energy costs [2–10].

Primary and secondary amines react with CO_2 in aqueous solutions to form carbamate or bicarbonate anions [8, 11].

$$2R^1R^2NH + CO_2 \leftrightarrow R^1R^2NCOO^- + R^1R^2NH_2^+ \quad (1)$$

$$R^1R^2NH + CO_2 + H_2O \leftrightarrow HCO_3^- + R^1R^2NH_2^+ \quad (2)$$

As shown in reactions (1) and (2), amines, protonated amines, carbamates, bicarbonates and water exist in the CO_2-loaded amine solutions. As the reaction rate, absorption capacity and heat of reaction differ between these two reactions, the branching ratio of these reactions is highly relevant to absorbent performance.

The steric hindrance of substituents adjacent to the amino group is a crucial factor which affects the product ratio of carbamate to bicarbonate anions, $[R^1R^2NCOO^-]/[HCO_3^-]$. For example, it is well-known that CO_2 absorbed in aqueous 2-amino-2-methyl-1-propanol (AMP) solutions predominantly exists as bicarbonate rather than carbamate, because of carbamate instability due to steric hindrance [11, 12].

There has been a tendency to only consider steric hindrance when discussing differences in reactivity toward CO_2 between different amine solvents [10]. However, because there is an abundance of amino lone pairs, hydroxyl groups,

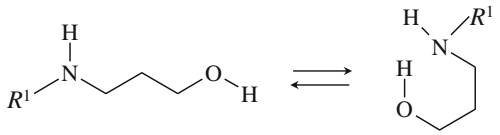

Fig. 1 Linear and hydrogen-bonded structures for primary and secondary amines from Puxty et al. [13]

ions and water in the system, it is conceivable that the reactivity is governed by other factors such as electron density, hydrogen bonding and solvation.

Puxty et al. [13] studied the CO_2 absorption of 76 amines and found seven amines with outstanding CO_2 absorption capacities. These seven amines shared a common structural feature: a hydroxyl group located within two or three carbons of the amino group. They inferred that intramolecular hydrogen bond formation between the amino and the hydroxyl groups (Fig. 1) might decrease the amine basicity to destabilize carbamate formation and push the absorption toward the more stoichiometrically efficient hydration pathway of reaction (2).

Because the hydrogen bond is of great importance in various aspects of chemistry, biology, and material science, there have been a number of quantum chemistry studies to understand and describe it [14–18]. For example, the intramolecular hydrogen bonding effects in salicylaldehyde derivatives were analyzed at the B3LYP/6−311+G(d,p) and MP2/aug-cc-pVDZ levels, where both levels of theory led to equivalent results [14].

In this work, we conducted quantum chemical (DFT) and spectroscopic (^{13}C-NMR) analyses to elucidate the molecular mechanisms underlying the CO_2 absorption products in aqueous alkanolamine solutions. We focused on the amine substituent effects in alkanolamine structures, $H(CH_2)_mNH(CH_2)_nOH$, by varying the alkyl chain length (m=2, 3, 4) and the alcohol chain length (n=2, 3, 4) to investigate the intramolecular hydrogen bond effects.

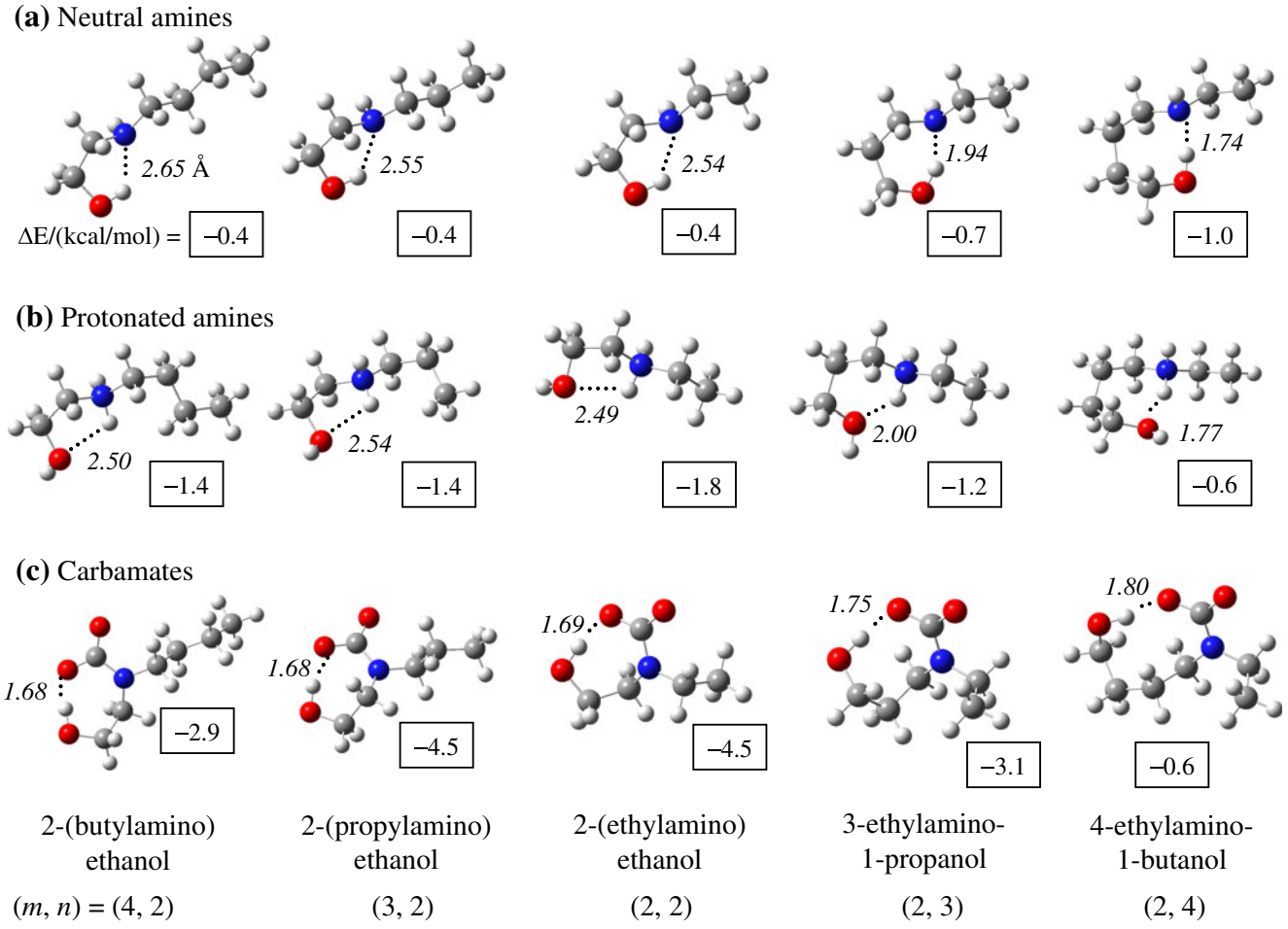

Fig. 2 Intramolecular hydrogen-bonded conformers for (a) neutral amine ($H(CH_2)_mNH(CH_2)_nOH$), (b) protonated amine and (c) carbamate with electronic energies (kcal mol^{-1}) relative to those of the linear conformers in Fig. 3. Intramolecular hydrogen bonds are indicated by dotted lines with lengths (Å) calculated at the SMD/IEF-PCM/B3LYP/6−311++G(d,p) level

Methodology

The electronic energy and the Gibbs free energy for all molecules in reactions (1) and (2) were calculated for the aqueous solutions of alkanolamine, $H(CH_2)_mNH(CH_2)_nOH$. For this purpose, DFT calculations with the SMD solvation model using the integral equation formalism polarizable continuum model (IEF-PCM) protocol for bulk electrostatics [19, 20] were carried out at the B3LYP/6−311++G(d,p) level. The free energy of each species in the aqueous solution phase was calculated based on the DFT geometry optimized structures followed by a frequency analysis for thermal and zero point energy corrections. From the frequency analysis, we confirmed that minimum energy structures were obtained for all optimized geometries in the aqueous solution phase.

SMD is the latest model to predict solvation free energies of neutral and ionic solutes in solutions [20]. This model separates the solvation free energy into two main components: one based on a self-consistent reaction field treatment of bulk electrostatics and the other non-electrostatic contribution arising from short-range interactions between the solute and solvent molecules. The SMD model has been parameterized using the IEF-PCM protocol mainly with the B3LYP hybrid functional. Recently we have used the SMD/IEF-PCM/B3LYP/6−311++G(d,p) level of theory to determine the reaction pathways of CO_2 absorption into aqueous AMP solutions [7].

In the free-energy calculations, a conductor-like screening model for real solvents (COSMO-RS) [21–24] was also applied with DFT at the BP/TZVP level. In this method, the distribution functions of the polarization charges on each molecular surface are obtained by applying the continuum solvation model in the conductor limit. Then, the free energy of each species in solution is calculated from its chemical potential with a statistical thermodynamics algorithm which measures the system affinity to molecular surface polarity. With the COSMO-RS/BP/TZVP method, we have developed a calculation model to predict the product ratio between carbamate and bicarbonate [8].

To investigate conformational effects, we performed a conformational distribution analysis for each species in the gas phase using molecular mechanics with the MMFF force field [25]. Based on the conformational analysis results, two types of stable conformations, intramolecular hydrogen bonding and linear, were set as the initial geometries in all DFT calculations.

Gaussian09 (Rev. A.1) [26], COSMOtherm (Ver. C2.1), TmoleX (Ver. 2.0) and Spartan'06 (Ver. 112) programs were used for the above calculations.

To measure the product ratio between carbamate and bicarbonate, CO_2 saturated samples were prepared by flowing 20 % CO_2 gas balanced with N_2 into a 30 wt.% aqueous amine solution in a glass scrubbing bottle at 40 °C. ^{13}C-NMR spectra were recorded at 100 MHz with a NMR spectrometer (JNM-ECA400, JEOL). To improve the lock

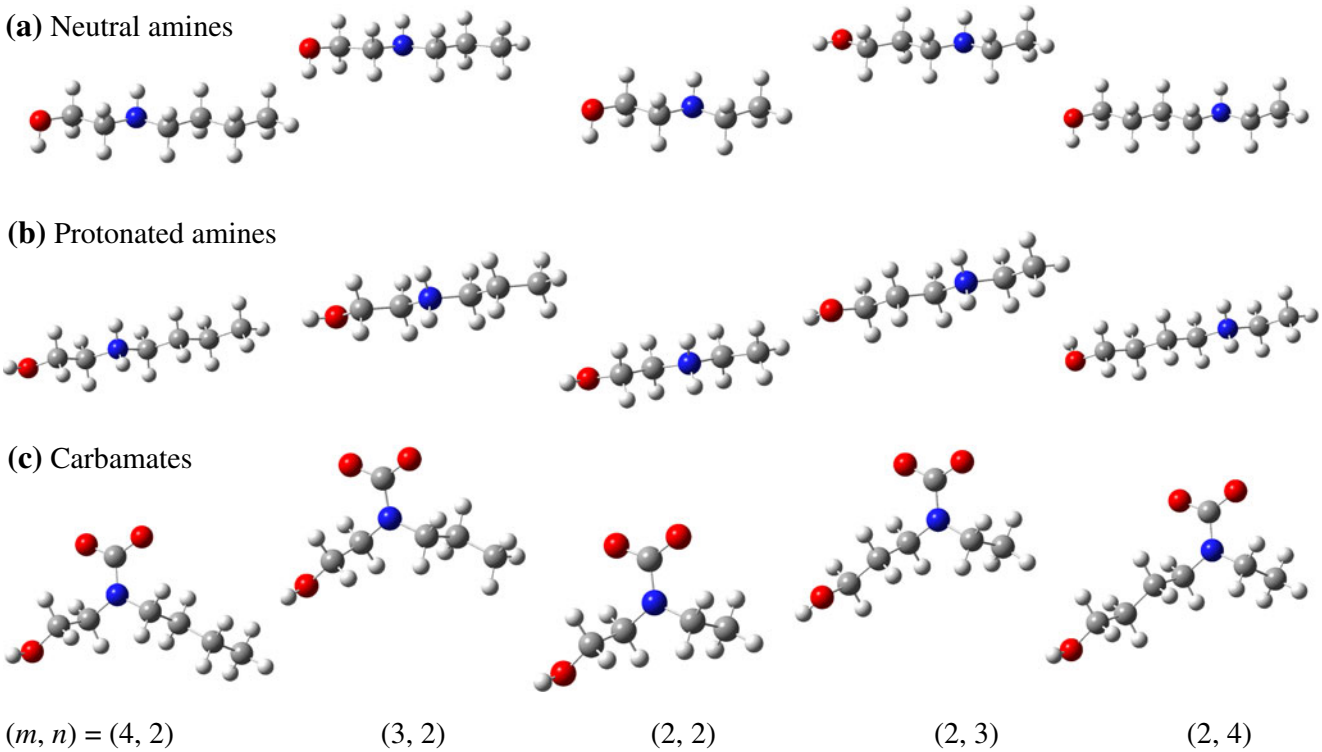

Fig. 3 Linear conformers for (a) neutral amine ($H(CH_2)_mNH(CH_2)_nOH$), (b) protonated amine and (c) carbamate

signal, 100 mL D_2O was added to 500 mL of each sample. Quantitative spectra were obtained at 21–23 °C using the inverse-gated decoupling technique with a pulse angle of 30°, a delay time of 30 s and 400 scans [8].

Results and discussion

For all species investigated, the most stable conformations, as determined with the MMFF force field in the gas phase, were those involving intramolecular hydrogen bonds (Fig. 2). The intramolecular hydrogen bonds of HN · · · HO, NH_2^+ · · · OH, and $NCOO^-$ · · · HO for neutral alkanolamine, protonated alkanolamine and carbamate, respectively, stabilize the molecular structures. Based on PCM and SM5.4A solvation calclations, it has been suggested that such intramolecular hydrogen bonds are favored even in amine–H_2O–CO_2 solutions [27].

Figure 2 shows the electronic energies relative to those of the corresponding linear conformers shown in Fig. 3. The negative relative energies of all conformers in Fig. 2, which were calculated using SMD/IEF-PCM/B3LYP/6-311++G(d,p) optimizations, indicate that the stabilization due to intramolecular hydrogen bonds is significant in aqueous solution. The carbamates are considerably stabilized in the amine species, and the stabilization energy is highly sensitive to the alcohol chain length.

Figure 2 also shows the intramolecular hydrogen bond lengths of HN · · · HO, NH_2^+ · · · OH, and $NCOO^-$ · · · HO in the SMD/IEF-PCM/B3LYP/6−311++G(d,p) optimized geometries. The intramolecular hydrogen bond lengths show negligible changes with alkyl chain length; however they are strongly dependent on the alcohol chain length. In the neutral and protonated alkanolamines, the intramolecular hydrogen bond length decreases with increasing alcohol chain length. In contrast, in the carbamates, the intramolecular hydrogen bond length increases with increasing alcohol chain length; this is in good agreement with the relative energies shown in Fig. 2, which reflect the extent of carbamate stabilization. These results predict that the product ratio of carbamate to bicarbonate will be reduced with increasing alcohol chain length.

We confirm the above prediction by quantitative ^{13}C-NMR measurements. In ^{13}C-NMR spectra of CO_2-loaded aqueous alkanolamine solutions, absorbed CO_2 are observed in the range 160–165 ppm [28, 29]. In Figs. 4 and 5, the peaks of 163–164 represent the carbonyl carbons of carbamate. The carbamates were unambiguously identified, because a carbamate molecule contains several carbon atoms.

From ^{13}C-NMR peaks, it is not possible to distinguish between protonated and proton-dissociative states, because of the fast proton-exchange rates. Consequently, the ^{13}C-peaks shift depending on the pH. A study on the pH dependency of the peak chemical shifts for CO_3^{2-} and HCO_3^-

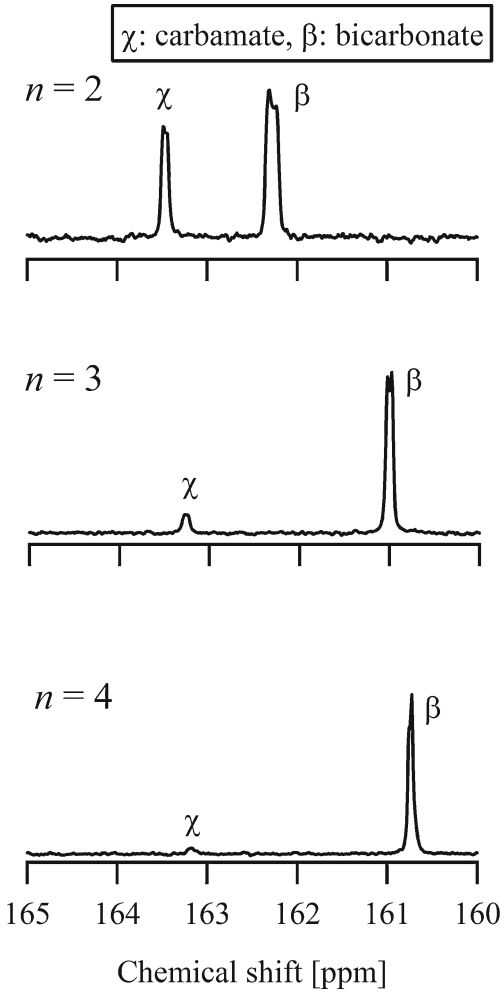

Fig. 4 ^{13}C-NMR spectra of CO_2 saturated 30 wt.% aqueous solutions of ethylaminoalkanol, $CH_3CH_2NH(CH_2)_nOH$ with alcohol chain lengths of 2, 3 and 4

reported that the peak shifts in samples solely containing CO_3^{2-} or HCO_3^- were 168.9 and 161.4 ppm, respectively [29]. Therefore, the peaks of 161–162 ppm in Figs. 4 and 5 are attributed to HCO_3^-.

Figure 4 clearly indicates that the formation of carbamate is markedly reduced in the propanolamine (n=3) and butanolamine (n=4) solutions, while a significant amount of carbamate is formed in the ethanolamine (n=2) solution. This confirms the prediction by DFT calculations. Furthermore, as shown in Fig. 5, the product ratios of carbamate to bicarbonate are comparable in the ethylethanolamine, propylethanolamine, and butylethanolamine solutions (m=2, 3, 4). These facts strongly suggest that the formation of carbamate or bicarbonate cannot be solely explained by the steric hindrance of substituents adjacent to the amino group. The alcohol chain length significantly affects the properties of CO_2 absorption by alkanolamine solutions.

The carbamate and bicarbonate equilibrium ratio is represented by the equilibrium constants of reactions (1) and

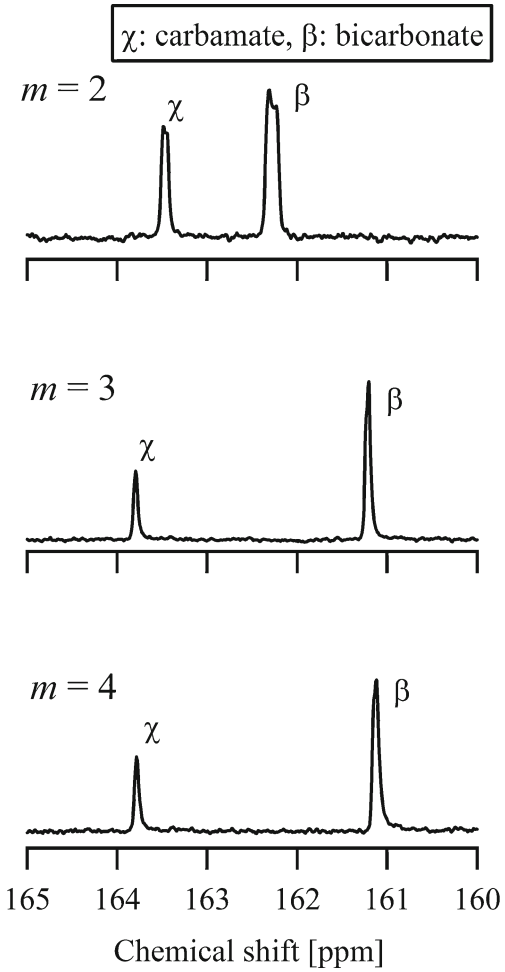

Fig. 5 ^{13}C-NMR spectra of CO_2 saturated 30 wt.% aqueous solutions of alkylethanolamine, $H(CH_2)_mNH(CH_2)_2OH$ with the alkyl chain lengths of 2, 3 and 4

(2), which are related to the reaction free energies. The ratio depends not only on the reaction free energies but also on the amine basicity, the chemical activities, and the pH [8].

Table 1 Reaction free energies (kcal mol^{-1}) of the CO_2 absorption by alkanolamines with the formation of carbamate (ΔG_1) and bicarbonate (ΔG_2) at 298.15 K and infinite dilution in water calculated at the SMD/IEF-PCM/B3LYP/6−311++G(d,p) and COSMO-RS/BP/TZVP levels of theory using the intramolecular hydrogen-bonded conformers

$H(CH_2)_mNH(CH_2)_nOH$ (m, n)	SMD/IEF-PCM/B3LYP/6311++G(d,p)		COSMO-RS/BP/TZVP	
	ΔG_1	ΔG_2	ΔG_1	ΔG_2
2-(butylamino)ethanol (4, 2)	1.07	2.49	−18.8	−16.2
2-(propylamino)ethanol (3, 2)	0.97	2.24	−18.8	−16.3
2-(ethylamino)ethanol (2, 2)	0.28	1.53	−20.1	−17.7
3-ethylamino-1-propanol (2, 3)	0.79	0.91	−15.4	−15.8
4-ethylamino-1-butanol (2, 4)	3.77	1.43	−10.7	−15.0

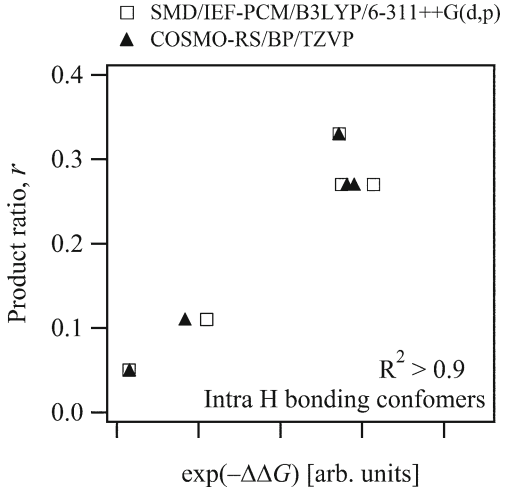

Fig. 6 Plot of the product ratio of carbamate to bicarbonate measured by ^{13}C-NMR in the CO_2 saturated aqueous alkanolamine solutions versus exp(−$\Delta\Delta G$). $\Delta\Delta G$ is the reaction free energy difference between formations of (1) carbamate and (2) bicarbonate, calculated by the solvation model coupled with DFT using the intramolecular hydrogen-bonded conformers

However, because of the structural similarity of the alkanolamines investigated in this work, we assume that the ratio has a linear relationship with an exponential function of the difference of reaction free energies:

$$r = \left[R^1R^2\mathrm{NCOO}^-\right]/\left[\mathrm{HCO_3}^-\right] = \mathrm{A}\ \exp(-\Delta\Delta G) + \mathrm{B} \quad (3)$$

$$\Delta\Delta G = \sigma(\Delta G_1 - \Delta G_2), \quad (4)$$

where σ is a scaling coefficient. The ratios of carbamate to bicarbonate can be experimentally determined from the peak area ratios in the ^{13}C-NMR spectra.

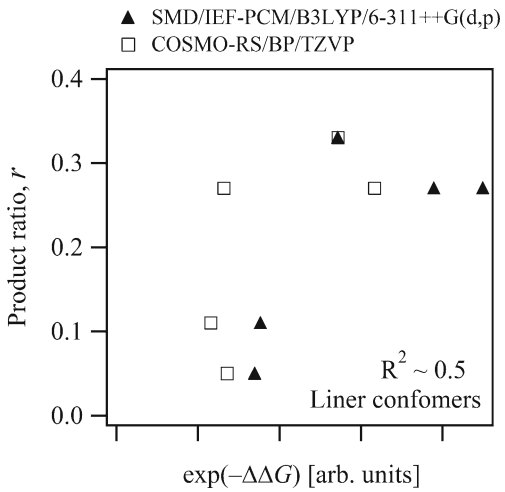

Fig. 7 Plot of the product ratio of carbamate to bicarbonate measured by ^{13}C-NMR in the CO_2 saturated aqueous alkanolamine solutions versus exp(−$\Delta\Delta G$). $\Delta\Delta G$ is calculated using the linear confomers

Table 1 shows the reaction free energies calculated at the SMD/IEF-PCM/B3LYP/6−311++G(d,p) and COSMO-RS/BP/TZVP levels. Although the values differ between the two levels of theory, the difference of reaction free energies are well linearly correlated between the two levels with a high coefficient of determination (R^2=0.99). For convenience, the scaling coefficient (σ) was determined for each level of theory in such a way that the scaled values of the reaction free energy difference in 2-(ethylamino)ethanol equal to each other at the two levels of theory.

The product ratios in the aqueous alkanolamine solutions obtained from the NMR spectra in Figs. 4 and 5 are fitted to Eq. 3 using the calculated values of reaction free energies at 298.15 K and are shown in Figs. 6 and 7. In Fig. 6, the experimental data correlate well with the calculated free energies using intramolecular hydrogen-bonded conformers at both the SMD/IEF-PCM/B3LYP/6−311++G(d,p) and COSMO-RS/BP/TZVP levels, with coefficients of determination 0.91 and 0.94, respectively. In contrast, the DFT calculations based on the linear conformers have reduced coefficients of determination, 0.44 for SMD and 0.53 for COSMO-RS (Fig. 7). With these results, we show that the intramolecular hydrogen bonds in amine−H_2O−CO_2 systems play a critical role.

Table 1 summarizes the free energies of reactions (1) and (2) calculated using the intramolecular hydrogen-bonded conformers. As seen, the free energies differ among the alkanolamines mainly in reaction (1). The stabilization energies are sensitive to the alcohol chain length of carbamate (Fig. 2). Therefore, especially the intramolecular hydrogen bonding of carbamate is considered to play an important role in amine−H_2O−CO_2 systems.

The calculated free energies are in good agreement with the experimental data, because both the SMD and COSMO-RS methods exceed conventional dielectric continuum solvation models in terms of adequate modeling of hydrogen bonds [20, 21].However, the effects of intermolecular hydrogen bonding, which may play a role, as well as intramolecular hydrogen bonds, are not clear in this work. Therefore, we cannot rule out the possibility of contributions of intermolecular hydrogen bonding to the experimental data. We investigated the effect of an explicit water molecule in the AMP−H_2O−CO_2 system and found that it did not significantly affect the reactivity with CO_2 [7]. In order to examine the intermolecular hydrogen bonding contributions, however, a large number of explicit molecules have to be treated. For a comprehensive understanding of the absorption mechanism, quantum mechanical/Monte Carlo/free-energy perturbation (QM/MC/FEP) study using large number of water molecules [30] is currently underway.

Conclusions

The reactions of CO_2 absorption in aqueous solutions of alkanolamine, $H(CH_2)_mNH(CH_2)_nOH$, have been studied at the SMD/IEF-PCM/B3LYP/6−311++G(d,p) and COSMO-RS/BP/TZVP levels, paying attention to the dependence of alkyl chain length (m=2, 3, 4) and alcohol chain length (n=2, 3, 4). The calculations have shown that intramolecular hydrogen bonds, especially the $NCOO^- \cdots HO$ bond in carbamate, significantly modify the aqueous solution phase and the product yields of CO_2 absorption are significantly affected by the alcohol chain length. Our calculations have been quantitatively validated by ^{13}C-NMR spectroscopy.

Acknowledgments This work was financially supported by the COURSE 50 project founded by the New Energy and Industrial Technology Development Organization, Japan.

References

1. Rochelle GT (2009) Amine scrubbing for CO_2 capture. Science 325:1652–1654
2. Rochelle G, Chen E, Freeman S, Wagener D, Xu Q, Voice A (2011) Aqueous piperazine as the new standard for CO_2 capture technology. Chem Eng J 171:725–733
3. Maiti A, Bourcier WL, Aines RD (2011) Atomistic modeling of CO_2 capture in primary and tertiary amines—heat of absorption and density changes. Chem Phys Lett 509:25–28
4. Robinson K, McCluskey A, Attalla M (2011) An FTIR spectroscopic study on the effect of molecular structural variations on the CO_2 absorption characteristics of heterocyclic amines. ChemPhysChem 12:1088–1099
5. Goto K, Okabe H, Chowdhury F, Shimizu S, Fujioka Y, Onoda M (2011) Development of novel absorbents for CO_2 capture from blast furnace gas. Int J Greenhouse Gas Control 5:1214–1219
6. Yamada H, Matsuzaki Y, Okabe H, Shimizu S, Fujioka Y (2011) Quantum chemical analysis of carbon dioxide absorption into aqueous solutions of moderately hindered amines. Energy Procedia 4:133–139
7. Yamada H, Matsuzaki Y, Higashii T, Kazama S (2011) Density functional theory study on carbon dioxide absorption into aqueous solutions of 2-amino-2-methyl-1-propanol using a continuum solvation model. J Phys Chm A 115:3079–3086
8. Yamada H, Shimizu S, Okabe H, Matsuzaki Y, Chowdhury F, Fujioka Y (2010) Prediction of the basicity of aqueous amine solutions and the species distribution in the amine−H_2O−CO_2 system using the COSMO-RS method. Ind Eng Chem Res 49:2449–2455
9. McCann N, Phan D, Wang X, Conway W, Burns R, Attalla M, Puxty G, Maeder M (2009) Kinetics and mechanism of carbamate formation from CO_2(aq), carbonate species, and monoethanolamine in aqueous solution. J Phys Chem A 113:5022–5029
10. da Silva EF, Svendsen HF (2007) Computational chemistry study of reactions, equilibrium and kinetics of chemical CO_2 absorption. Int J Greenhouse Gas Control 1:151–157
11. Vaidya PD, Kenig EY (2007) CO_2—alkanolamine reaction kinetics: a review of recent studies. Chem Eng Technol 30:1467–1474
12. Chakraborty AK, Astarita G, Bischoff KB (1986) CO_2 absorption in aqueoussolutions of hinderedamines. Chem Eng Sci 41:997–1003

13. Puxty G, Rowland R, Allport A, Yang Q, Bown M, Burns R, Maeder M, Attalla M (2009) Carbon dioxide postcombustion capture: A novel screening study of the carbon dioxide absorption performance of 76 amines. Environ Sci Technol 43:6427–6433
14. Jezierska-Mazzarello A, Szatyłowicz H, Krygowski TM (2012) Interference of H-bonding and substituent effects in nitro- and hydroxy-substituted salicylaldehydes. J Mol Model 18:127–135
15. Zawada A, Kaczmarek-Kędziera A, Bartkowiak W (2012) On the potential application of DFT methods in predicting the interaction-induced electric properties of molecular complexes. J Mol Model 18:3073–3086
16. Nagaraju M, Sastry GN (2011) Effect of alkyl substitution on H-bond strength of substituted amide-alcohol complexes. J Mol Model 17:1801–1816
17. Oliveira BG, Araújo RCMU, Carvalho AB, Ramos MN (2009) A chemometrical study of intermolecular properties of hydrogen-bonded complexes formed by $C_2H_4O \cdots HX$ and $C_2H_5N \cdots HX$ with X = F, CN, NC, and CCH. J Mol Model 15:421–432
18. Delchev VB, Mikosch H (2006) DFT study of the gas phase proton transfer in guanine assisted by water, methanol, and hydrogen peroxide. J Mol Model 12:229–236
19. Tomasi J, Mennucci B, Cammi R (2005) Quantum mechanical continuum solvation models. Chem Rev 105:2999–3093
20. Marenich AV, Cramer CJ, Truhlar DG (2009) Universal solvation model based on solute electron density and on a continuum model of the solvent defined by the bulk dielectric constant and atomic surface tensions. J Phys Chem B 113:6378–6396
21. Klamt A (2011) The COSMO and COSMO-RS solvation models. WIREs Comput Mol Sci 1:699–709
22. Eckert F, Klamt A (2006) Accurate prediction of basicity in aqueous solution with COSMO-RS. J Comput Chem 27:11–19
23. Eckert F, Klamt A (2004) Fast solvent screening via quantum chemistry: COSMO-RS approach. AICHE J 48:369–385
24. Klamt A, Jonas V, Burger T, Lohrenz JCW (1998) Refinement and parameterization of COSMO-RS. J Phys Chem A 102:5074–5085
25. Francl MM (1985) Polarization corrections to electrostatic potentials. J Phys Chem 89:428–433
26. Frisch MJ, Trucks GW, Schlegel HB, Scuseria GE, Robb MA, Cheeseman JR, Scalmani G, Barone V, Mennucci B, Petersson GA, Nakatsuji H, Caricato M, Li X, Hratchian HP, Izmaylov AF, Bloino J, Zheng G, Sonnenberg JL, Hada M, Ehara M, Toyota K, Fukuda R, Hasegawa J, Ishida M, Nakajima T, Honda Y, Kitao O, Nakai H, Vreven T, Montgomery JA Jr, Peralta JE, Ogliaro F, Bearpark M, Heyd JJ, Brothers E, Kudin KN, Staroverov VN, Kobayashi R, Normand J, Raghavachari K, Rendell A, Burant JC, Iyengar SS, Tomasi J, Cossi M, Rega N, Millam NJ, Klene M, Knox JE, Cross JB, Bakken V, Adamo C, Jaramillo J, Gomperts R, Stratmann RE, Yazyev O, Austin AJ, Cammi R, Pomelli C, Ochterski JW, Martin RL, Morokuma K, Zakrzewski VG, Voth GA, Salvador P, Dannenberg JJ, Dapprich S, Daniels AD, Farkas Ö, Foresman JB, Ortiz JV, Cioslowski J, Fox DJ (2009) Gaussian 09, Rev A1. Gaussian Inc, Wallingford
27. da Silva EF, Svendsen HF (2003) Prediction of the pK_a values of amines using ab initio methods and free-energy perturbations. Ind Eng Chem Res 42:4414–4421
28. Böttinger W, Maiwald M, Hasse H (2008) Online NMR spectroscopic study of speciesdistribution in MEA−H_2O−CO_2 and DEA −H_2O−CO_2. Fluid Phase Equilibria 263:131–143
29. Jakobsen JP, Krane J, Svendsen HF (2005) Liquid-phase composition determination in CO_2−H_2O−alkanolamine systems: An NMR study. Ind Eng Chem Res 44:9894–9903
30. Hori K, Yamaguchi T, Uezu K, Sumimoto M (2011) A free-energy perturbation method based on Monte Carlo simulations using quantum mechanical calculations (QM/MC/FEP method): Application to highly solvent-dependent reactions. J Comput Chem 32:778–786